



Collagen biology meets medical device technology: current reality, future dreams

James San Antonio¹, Anton Persikov², Jessica Stevens³, Olena Jacenko⁴ and Joseph Orgel⁵

¹Global Quality and Operations, Stryker, Inc., 45 Great Valley Parkway, Malvern, PA 19355, USA, 484-323-8802; james.sanantonio@stryker.com

²Lewis-Sigler Institute for Integrative Genomics, Princeton University, Carl Icahn Lab, Princeton, NJ 08544, USA, 609-258-7195; persikov@princeton.edu

³Research and Development, Stryker Spine Orthobiologics, Inc. 77 Great Valley Parkway, Malvern, PA 19355, USA; 610-407-5203, jessica.stevens@stryker.com

⁴Department of Biomedical Science, School of Veterinary Medicine, University of Pennsylvania, 3800 Spruce Street, Philadelphia, PA 19104, USA, 215-573-9447; jacenko@vet.upenn.edu

⁵Pritzker Institute of Biomedical Science and Engineering, Illinois Institute of Technology, 3440 S. Dearborn, Chicago IL. 60616, USA, 312 567-3398; orgel@iit.edu

Abstract

Type I collagen, the predominant protein of vertebrates, assembles with other collagens and non-collagenous extracellular matrix molecules into large cable-like fibrils which help dictate the structure and function of tissues including skin, tendon, bone, and cornea. Collagen also has a myriad of uses in the manufacture of glues, leather, and formulations to promote health and beauty. To help decipher the structure and biology of this “cornerstone of life”, we examined type I collagen fibrils *in situ* by x-ray diffraction, establishing the molecular conformation and packing topology of triple helices within the microfibril (fibril subunit) and fibril. We also built an interactome to correlate the hundreds of functional domains, ligand binding sites, and human mutations mapping to the protein. The fibril was found to comprise two domains: one regulating cell interactions and fibril remodeling, and the other dictating structure, mediating proteoglycan binding, fibril crosslinking, and biomineralization. Insights from interactomes for type I collagen chemistry created here, and for type III collagen biology are also discussed. We also consider the present state and future promise of the multi-billion dollar collagen-based medical device industry, which supplies a huge portfolio of collagenous scaffolds and flowable formulations to correct tissue defects and promote healing. We propose how acquiring the abilities to fashion biocompatible collagen-based implants with requisite dimensions, tissue architecture, structural integrity, and *in vivo* longevities may rely on three emerging methods: collagen fibril alignment, 3D bioprinting, and the creation of genetically engineered “boutique” collagens with novel structural and biologic attributes.

Keywords: collagen, matrix, interactome, alignment, 3D printing, medical devices.

1 – Introduction

Collagens are among the most ubiquitous and complex of the extracellular matrix (ECM) molecules of vertebrates and invertebrates (Kadler et al., 2007; Marini et al., 2007; Piez and Reddi, 1984). At least thirty genetically distinct collagens have been discovered in the human. For most collagens, the majority of their sequence exists as a triple helix, which makes them unique among proteins. These domains are rigid, rope-like cylindrical structures which, depending on the collagen type, are

sometimes interspersed between small flexible non-triple helical regions, or larger, sometimes globular non-collagenous domains. The triple helical domains are composed of contiguous Gly-X-Y tripeptide repeats, with the obligate Gly as the only residue with a side chain small enough to fit within the coiled-coil of the triple helix. Type I collagen is the most abundant of the collagens and is a main focus of our research.

2 – Type I collagen structure and assembly

Type I collagen is synthesized by cells as $\alpha 1$ and $\alpha 2$ procollagen chains, each encoded by separate genes that are translated into proteins somewhat greater than 1000 amino acids long (Piez and Reddi, 1984). Domains on the C-terminal propeptides promote the polymerization of two $\alpha 1$ and one $\alpha 2$ chains into the procollagen triple helical monomer (Fig. 1, A and B). Extracellularly, N- and C-proteinases remove the globular termini of procollagen, and every 67 nm along the fiber axis, five monomers assemble in a quarter-staggered fashion to form part of the supramolecular “helix,” the microfibril. Each microfibril, the proposed subunit of the collagen fibril (Fig. 1, C–E), and its immediate microfibrillar neighbors are connected by N- and C-terminal intermolecular cross-links. The basic repeating morphological structure of the fibril is the D-period, 67 nm long, and composed of one overlap and one gap zone. Each D-period contains the complete monomer sequence derived from overlapping consecutive elements of five monomers (Fig. 1C, box). Other collagens, proteoglycans (PGs), and matrix macromolecules may assemble with the fibril to impart tissue-specific properties to the heterotypic polymer (Piez and Reddi, 1984; Scott, 1988).

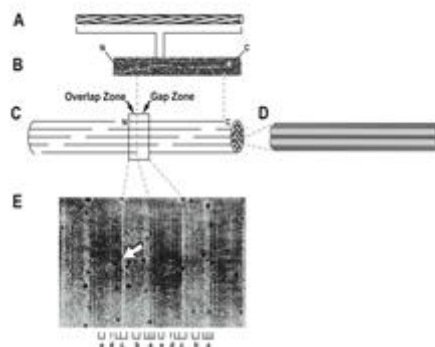


Figure 1. Type I collagen assembly and structure (see text). Reprinted with permission from Sweeney et al., 2008.

3 – X-ray diffraction elucidates collagen structure

In the last century, it was determined that fibrillar collagens show the iconic D-banding structure, and an organization along the fiber axis nearly parallel to the protein’s amino acid sequence. This ~67nm repeat in certain tissues, composed of closely spaced molecular triple-helices staggered from each other by the D repeat value, is so consistent that it produces X-ray diffraction to better than 0.4 nm resolution and is well-ordered to the point of single amino acid spacing (Orgel et al., 2006; Orgel et al., 2000). Yet, the three-dimensional position of individual amino acids is not known with high certainty (Orgel and Irving, 2014). Since the structure of interest is a protein array that is disrupted and fragmented to enable single crystal crystallography (thus destroying that structure), and is largely opaque to microscopy beyond 10 nm or so resolution (Orgel and Irving, 2014), direct observation of all amino acid positions is not possible, but in some cases has been accurately seen with advanced fiber diffraction techniques applied to native tendon collagen *in situ*. Thus, heavy atom labeling employing iodine salts was used to localize Tyr residues that are only found in the telopeptides the collagen chains (which border the gap-overlap D-period divisions) for type I collagen (Orgel et al.,

2000). This helped determine the size of the gap-overlap regions, and the locations of specific sections of the collagen sequence from which the remainder of the sequence was estimated from information gleaned via structural analyses of triple helical peptide collagen models (Orgel et al., 2006; Rainey and Goh, 2002). Direct visualizations of heavy atom-labeled amino acids provided an accuracy of better than 0.5 nm resolution. Moreover, these methods helped produce a three-dimensional structure of the collagen triple helix and its packing arrangement within the fibril (Fig 2) (Orgel et al., 2006; Rainey and Goh, 2002). At around 1.1 nm in resolution as viewed by macromolecular fiber diffraction the bulk shape or “outline” of the helix is marginally defined although in general the side chains of its constituent amino acids cannot be visualized. Yet, regions of electron density were seen stretching between helices in the vicinity of where the long side chains of amino acids such as Lys and Arg were estimated to be located, based on fitting of triple helix models to the electron density patterns seen by fiber diffraction and single crystal crystallography (Orgel et al., 2006).

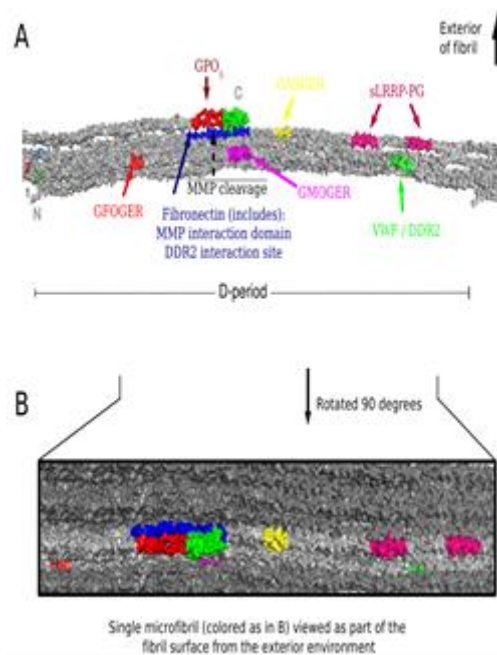


Figure 2. A. X-ray diffraction image shows “worm tracings” of the five triple helices of the type I collagen microfibril. Sequences for cell interactions (GFOGER); fibril remodeling; MMP cleavage; platelet binding/hemostasis (GPO₅); and fibril structure (decorin core protein binding site, sLRRP-PG) are indicated. B. From the fibril exterior, the microfibril from panel A (light gray) and surface accessibilities of its biologically relevant sequences are shown.

The X-ray diffraction structure of the molecular helix has been shown to be a superhelix, a right handed triple helix composed of three left-handed 'polyproline II' helices. The amino acid sequence, dominated by the GlyXY repeat assumes either of at least two helical symmetries (between 7/2 and 10/3), likely depending on features such as the identity of the amino acids occupying the X and Y positions, degree of hydration, helix strain and the lateral packing and interactions between neighboring triple helices. Precise structural determination awaits higher resolution fiber X-ray diffraction data of the natural material (not just collagen peptide fragments), which the authors have recently collected to around 0.3 nm resolution (Barrea et al., 2014; Orgel et al., 2014). Such data will soon enable precise identification of the positions of most if not all of the amino acids within the molecular packing comprising the fibril, including the polarity of each alpha chain that remains uncertain.

Finally, the X-ray diffraction structure also shows type I collagen, and likely related fibrillar collagens, to possess a microfibrillar composite structure, where the D-staggered molecules pack closely in a helix-like right-handed wound-structure every 4.46D, the approximate length of a collagen molecule.

Arrays of microfibrils are wound around a central point to form collagen fibrils, while the packing of the microfibrils is precise enough that the composite molecules form a quasi-hexagonal lattice with an average molecule spacing of 1.3 nm. These fibrils are bridged with each other via PGs to form fibril-bundles that comprise large collagen fibers visible to the naked eye in animal tissues (Orgel et al., 2011).

4 – Collagen model suggests mechanisms of dinosaur peptide survival

The discovery by Dr. Mary Schweitzer that collagen peptides survived in exceptionally well preserved dinosaur fossils garnered international attention. Mapping the positions of the dinosaur peptides on our 3D collagen model revealed them to reside in the core, or more sheltered region of the microfibril (San Antonio et al., 2011). Moreover, the majority of the peptides aligned within several regions of the fibril, suggesting their preservation *en bloc*. Thus physical shielding by the protein and perhaps its associated biomineral likely resulted in the selective preservation of collagen fragments through deep geologic time.

5 – Collagen interactomes lend insights into collagen biology and chemistry

The first published map of type I collagen included its primary protein sequence and a proposed mechanism of charge-based polymerization consistent with the “quarter stagger” fibril structure (Chapman, 1974). The unique molecular structure of collagens allowed us to expand on that theme and construct collagen interactomes or “road maps” on which triple helices may be represented as 2D arrays of three linear polypeptide chains. Sequences are annotated with positions of sites mediating cell or ligand binding, proteolysis, amino acids associated with mutations, post-translational modifications, chemically-reactive groups, etc.

6 – Type I collagen biology

Our type I collagen interactome (Sweeney et al., 2008) includes over fifty known ligand binding sites and functional domains, and 600 human disease-associated mutations mapping to the protein, all of which were experimentally determined in hundreds of labs around the world, including our own. Analysis of patterns of ligand binding sites and mutation distributions revealed the collagen fibril to have two major domains (Sweeney et al., 2008) (Fig. 3). The dynamic aspects of collagen biology occur in one region, called the “Cell Interaction Domain”, which occupies much of the fibril’s overlap zone. The domain includes sequences mediating cell surface (integrin) receptor binding, bioactive factor ligation, collagen remodeling by vertebrate collagenase, angiogenesis (vascular regeneration and growth) and hemostasis (blood clotting). The remainder of the fibril comprises the “Matrix Interaction Domain”, where intermolecular crosslinking, structural macromolecules like the decorin PG bind, and mineralization are proposed to occur (via undefined sequences/mechanisms) in bone. Analysis of the locations of phenotypically severe mutations in the COL1A1 or COL1A2 genes (mostly manifest as Osteogenesis Imperfecta, or brittle bone disease) associated with embryonic lethality or death, has defined a subset of collagen sequences with crucial roles in protein structure and human biology (Marini et al., 2007).

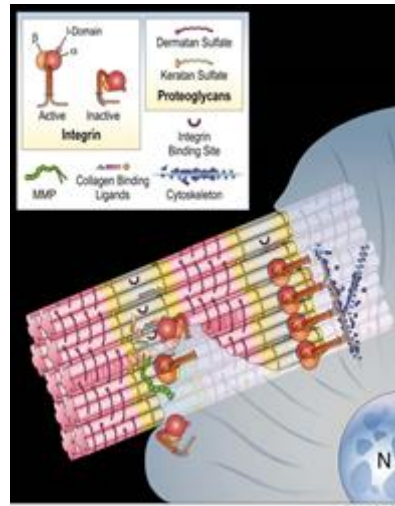


Figure 3. Interactome helps visualize dynamic collagen biology. Cell interacts with collagen fibril's cell interaction domain via integrins. The matrix interaction domain hosts proteo-glycans, intermolecular cross-links and biomineralization. Reprinted with permission from Sweeney et al., 2008.

Many questions remain in type I collagen biology. How does the collagen fibril polymerize, and during fibril assembly, tissue-specific function(s), and remodeling, which sequences are on the outside, or inside of the fibril? Answering such questions may lead to the design of agents to inhibit pathological collagen deposition; e.g., in liver fibrosis, and for controlling collagen fibril assembly in medical device manufacturing. Which collagen sequences nucleate hydroxyapatite crystal growth during bone mineralization? Elucidating such mechanisms may lead to therapeutic interventions to combat pathological mineralization e.g., in osteoporosis, and guide the *ex vivo* mineralization of tissue engineered bone, and the design of genetically engineered “boutique collagens” with enhanced (for bone replacement) or diminished (for soft tissue substitutes) mineralization capacities. Future collagen structure-function investigations may best exploit methods to selectively label solvent-exposed fibril surfaces (e.g., those unoccupied by mineral), and identify labeled collagen peptide sequences by Mass Spectrometry.

7 – Type I collagen chemistry

A collagen map constructed by Dr. Eckhardt Heidemann- in honor of whom this lecture is named- illustrated the positions of chrome and aldehyde-reactive amino acids on the $\alpha 1(I)$ chain relative to the D-period overlap and Gly-Pro-Pro triplets for the interest of leather chemists (Heidemann, 1988). Here we updated his map (Fig. 4) to include both α chains, annotated to highlight facets of collagen structure (see refs. (Heidemann, 1988) (Covington, 2009; Sweeney et al., 2008) (Fernandes et al., 2011; Gautieri et al., 2014; Hu et al., 1997; Hudson and Eyre, 2013; Morello et al., 2006; Stachel et al., 2010) for the following), including 1) amino acid side chain chemistries: chrome-reactive residues Glu and Asp, aldehyde reactive and basic Lys, basic Arg; Asn and Gln that undergo amide side-chain hydrolysis during liming; Lys modified by non-enzymatic glycation; and Lys-Arg pairs proposed as substrates for crosslinking via glucosepane; and those strongly hydrophobic; 2) reactive residues/sequences for: transglutaminase crosslinking (Gln and Lys), and MMP-1 cleavage for fibril remodeling; 3) those relevant to fibril supramolecular structure: zone of “detergent fracture” induced, e.g., by Triton X-100 treatment; Gly-Pro-Pro triplets conferring triple helix rigidity, and atypical triplets (e.g., Gly-Ala-Ala), low stability/flexibility (see type III interactome section); hydroxy-Lys native intermolecular crosslinks; and 3-hydroxy-Pro (most other Pro are 4-hydroxy) crucial for human bone structure; and 4) decorin PG binding region, and the cell interaction domain, as reference points to the collagen biology interactome. A cursory examination of the map suggests a diversity of unique

sequences distributed throughout the triple helix. Distribution of individual amino acid types is also non-homogeneous, e.g., on the D-period, several fibril regions contain many Lys-Arg pairs capable of forming advanced glycation end products; whereas others, e.g., in the central gap zone, lack them altogether. Moreover, the number of Gln residues in the overlap zone is about twice that of the gap zone, etc.

To complement experimental and theoretical studies on mechanisms of leather tanning (Swamy et al., 2011) (King et al., 1996), it may be useful to create a user-friendly database wherein fibril chemistry can be viewed in the 3D native conformation; e.g., before and after alkaline modification (liming), intermolecular crosslinking via chrome, glucosepane, or transglutaminase action, detergent fracture on accessibility/location of chrome-reactive groups, etc. The collagen chemistry and biology interactomes should also be correlated to identify the structural/chemical features of collagen associated with its crucial biological functions.

8 – Type III collagen

Our ongoing research also probes the biological and physical nature of type III collagen that comprises a significant proportion of the hide protein of calf and other young animals. Type III collagen is a fibrillar collagen important in embryogenesis (Rong et al., 2008), hemostasis (Ottani et al., 2001), and wound healing (Lehto et al., 1985; Oliveira et al., 2010), and is proposed to play a critical structural role in blood vessels and distensible organs, such as the large bowel and uterus. Mutations in the collagen III human gene, COL3A1, may result in Ehlers-Danlos syndrome type IV characterized by extensive bruising, and sometimes organ or vascular rupture (Pepin et al., 2000). Construction of an interactome of the collagen III $\alpha 1$ homotrimer is underway (Parkin et al.). Preliminary data reveal that type III collagen has a similar functional domain structure to collagen I, but with enhanced hemostasis functions.

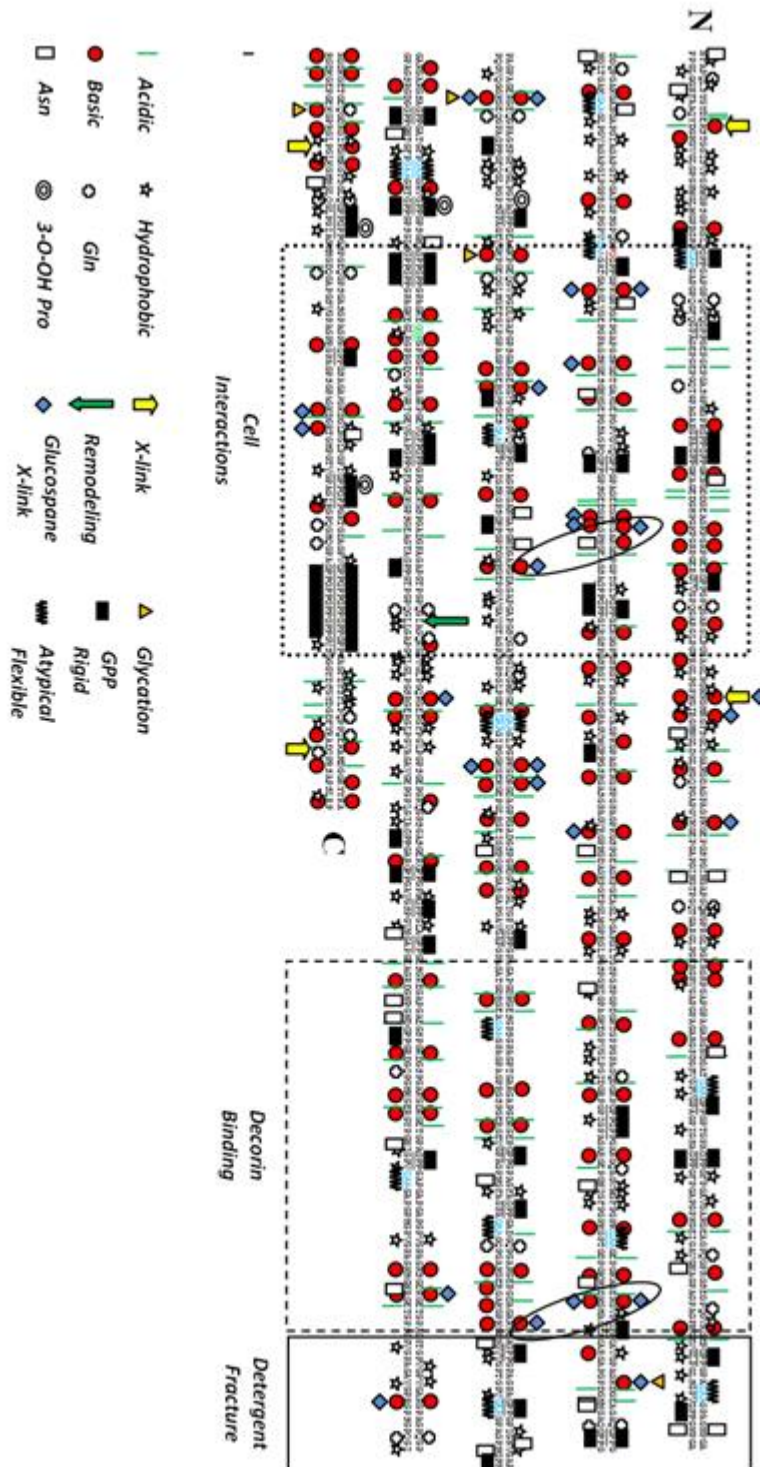


Figure 4. Type I collagen chemistry interactome. The primary amino acid sequences of human collagen were from genbank and aligned according to Dr. Chapman's overlap model. Map annotations are as in text and figure legend. Two of the many possible Lys-Arg glucosepane crosslinks are enclosed by ellipses.

Type III collagen has higher Gly, and lower Pro contents by about two percent than other fibrillar collagens (Piez and Reddi, 1984) and nearly twice the number of "atypical triplets", e.g., Gly-Ala-Ala or Gly-Gly-Y than type I (Parkin et al.). Gly-Pro-Pro-rich regions promote triple-helical rigidity with

more compact 7/2 symmetry, while non-Pro residues alter the triple helical twist (Brodsky and Persikov, 2005).

Moreover, while Gly-Pro-Pro triplets are the main contributors to triple-helix stability, atypical triplets are destabilizing (Persikov and Brodsky, 2002; Persikov et al., 2000). Thus, atypical triplets contribute to low triple helical stability and structural flexibility compared to Gly-Pro-Pro, the most stable collagen triplet. We asked if the distribution of atypical triplets in type III collagen is random, and if not, where domains of greater, and lower stability may exist on the protein. We looked for cross-correlation of occurrences of atypical triplets and Gly-Pro-Pro triplets in the overlapping D-period regions. The positions of atypical and Gly-Pro-Pro triplets were binned into ten regions of equal size. We observed that atypical and Gly-Pro-Pro triplets predominated in different regions of the molecule (data not shown). To further study the effect of Gly-Pro-Pro and atypical triplets on the stability of type III collagen we used the Collagen Stability Calculator (Persikov et al., 2005). We observed co-localization of local stability variations, observing three major regions of decreased stability (Fig. 5). We thus propose type III collagen functions as a “Flexi-Rod” in which a confluence of atypical triplets creates flexible domains, allowing focal expansion or deformation of several discrete fibril regions (Fig. 5). The intervening rod-like domains may preserve the more rigid triple helical conformation to allow crucial functions like cell/ligand binding and proteolysis. Future work should determine if the flexibility inherent in type III collagen- based on its content and distribution of atypical triplets- may functionally relate to its predominance in distensible tissues, and whether type I and other fibrillar collagens behave like “Flexi-Rods” or display less flexibility/structural heterogeneity.

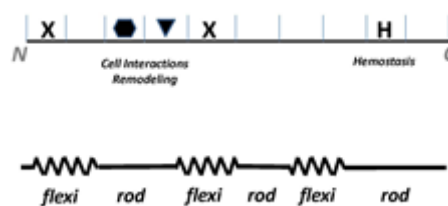


Figure 5. Top: Schematic of type III collagen monomer with sites for cell interactions and remodeling flanked by crosslinks (X) and hemostasis domain (H). Bottom: Stability modeling (see text) indicates clusters of atypical collagen sequences of lower stability (springs) are interspersed with rigid zones (rods) hosting crucial biologic functions.

9 – Collagen-based medical devices, current reality

Collagen-based medical devices comprise a multi-billion dollar market per year worldwide. Raw materials for such devices are most often derived from type I collagen-rich tissues like bovine or porcine skin, bone, tendon, bladder, or intestinal submucosa (Abou Neel et al., 2013). To satisfy regulatory agencies such as the US Food and Drug Administration requires stringent material sourcing and manufacturing controls to minimize the potential for contamination of the collagens, especially with pathogenic organisms. “Solid-phase” collagen processing methods reminiscent of those of the leather industry are the most commonly used and are simpler and less costly than “solution phase” purification approaches (e.g. see (Abou Neel et al., 2013; Friess, 1998; Komanowsky et al., 1978; Meyer and Schropfer, 2013) for review of the following). For the former, tissues may be manually trimmed/cleaned of extraneous tissue and subjected to rinses, and subjected to various treatments including liming/de-liming, organic solvent extraction protocols, heat denaturation, combined with physical processing like slicing, grinding, scaffolding, chemical cross-linking, and lyophilization, among others. The resultant preparations are depleted of cellular material and other contaminants such as blood, and usually composed of partially denatured to near-native meshworks of crosslinked collagen fibrils and in some cases additional ECM molecules and bioactive factors. Some materials instead are predominantly gelatin and/or its derivatives. Constructs are often sterilized by gamma

irradiation. They may comprise durable, fibrous sheets of various thicknesses used as wound overlays, or patches for the repair of tendons, bladders, hernias, or pelvic wall prolapse. In some cases, collagen or gelatin particle suspensions are obtained and processed into porous, biodegradable scaffolds of various shapes for the delivery of bone regeneration agents, as tubular conduits to promote reconnection of severed nerves, or sponge-like hemostats to promote blood clotting. The robust physical nature of such collagen scaffolds often conferred by native intermolecular crosslinks, imparts structural integrity to the devices; equally crucial are the biocompatible and biodegradable qualities of the collagen. In some cases the biologic activities of collagen also play prominent roles. For example, collagen-based hemostats may absorb liquid from blood thereby concentrating and activating clotting factors, and collagen contains several classes of binding sites for platelet aggregation and activation, which promote hemostasis.

In “solution phase” collagen processing, acids or proteases like pepsin are used to extract native collagens from tissues. Acid extracted collagen comprises native telopeptide-containing collagen monomers or small oligomers, rapidly polymerizes in response to phosphate precipitation, yet is potentially immunogenic owing to its telopeptide content. In contrast, pepsin-purified collagen is largely devoid of telopeptides making it slower to polymerize, yet is near-native and potentially safer for use in medical devices. Collagen solutions are settled to remove insoluble matter and non-collagenous contaminants, and bacterial, viral and prion (causative agent of Mad Cow disease) contents may be diminished many-fold by chemical treatments, and microbial bioburden further reduced by sterile filtration. Gamma irradiation is not possible as it denatures and renders the collagen insoluble. The collagen is phosphate-precipitated to form native-type fibrils, and concentrated which further removes contaminants. Re-suspended fibril suspensions are formulated to be syringe-extrudable and topically applied to diabetic wounds to promote healing, injected into the skin as dermal fillers to correct wrinkles or other defects, or combined with the blood clotting enzyme thrombin and applied to surgical sites to stop bleeding.

Despite the successes of modern collagen-based implants, many have limitations. Most do not closely mimic the native structure and function of the tissues they are intended to correct as they lack the appropriate ECM composition and architecture, complement of living cells, and capacity to become rapidly vascularized to support their *in vivo* survival and remodeling. The dimensions of devices derived from solid phase processing methods are limited by those of their source tissues- thus, load-bearing scaffolds cannot be fashioned from hide or tendon to replace large bones or bone pieces, nor can they be appropriately mineralized, necessitating the use of cadaver bone allografts. Last, although collagens derived from solution phase purification are the most native, biocompatible, and conformationally flexible, methods have not been developed to fashion these into native-type connective tissue substitutes having the appropriate structural integrity and target dimensions. However, two emerging technologies- collagen alignment and 3D bioprinting- may provide the means to fabricate next generation medical devices from such soluble collagen formulations.

10 – Collagen polymerization and alignment technologies

Collagen polymerization and aggregation occur in virtually all tissues where fibrils may become aligned and cross-linked together in tissue-specific configurations. For example, an arrangement of aligned collagen fibril bundles provides structural integrity and light transmittance to the cornea (Whitford et al., 2015), and tensile strength and a load-bearing capacity to tendons and bones (Piez and Reddi, 1984; Svensson et al., 2013). During embryogenesis, collagen fibrils may form templates for endothelial cell attachment culminating in capillary morphogenesis (Iruela-Arispe et al., 1991), and fibroblasts secrete and direct the assembly and alignment of collagen fibrils during tendonogenesis (Hay, 1991). The distribution, arrangement, size and density of collagen fibrils in animal hides is species-specific and may contribute significantly to the physical properties of leather (Basil-Jones et al., 2011; Osaki, 1999).

Collagen fibrillogenesis is a multi-stage process (Piez and Reddi, 1984) beginning with nucleation, where crosslinked collagen monomers (oligomers) form templates for fibril accretion. Next, fibril growth proceeds rapidly through lateral aggregation, and culminates when fibril growth slows appreciably, and mature collagen fibrils persist (Fig. 1). Variables including pH, ionic strength, temperature, and agents/conditions including proteoglycans, enzymatic processing, and lanthanides to name a few, influence fibrillogenesis kinetics and the morphology of the resultant fibrils (Evans and Drouven, 1983; Friess, 1998; Reigle et al., 2008; Wood and Keech, 1960). Thus, native fibrils containing telopeptides polymerize about twice as quickly as pepsinized collagen, and lanthanides increase the rate of nucleation and polymerization. A small subset of collagen sequences were proposed to play roles in fibrillogenesis (Prockop and Fertala, 1998). Yet, the precise mechanisms of fibrillogenesis remain unknown.

Methods have been developed align collagen fibrils into scaffolds *ex vivo*. Thus, application of a 20 Kilogauss magnetic field to collagen fibrils during heat gelation oriented the fibrils perpendicular to the field, forming scaffolds up to 2.5 mm thick (Murthy, 1984). Others subjected collagen gels to “flow orientation”— pressure-driven extrusion through apertures of about 0.4 mm from which collagen sheets, tubes, and meshes were formed. These structures, once dehydrated, had surface areas of up to about 2 cm², thicknesses ranging from about 10-100 microns, and birefringence indicative of collagen fibril alignment (Isobe et al., 2012). Similarly, hydrodynamic flow was used to assemble ultrathin, highly anisotropic ribbon-like structures on mica surfaces. The constructs were comprised of aggregates of collagen microfibrils less than 50 nanometers thick (Jiang et al., 2004). Another approach generated “Langmuir–Blodgett” films by immersing hydrophobic glass microscope slides into a collagen and propanol-containing solution, once or repeatedly to generate collagen films of up to 100 nm thick. Varying the dipping directions and slide geometries resulted in scaffolds exhibiting various patterns of collagen alignment as seen by bright field microscopy, and which were stable for several months at ambient temperatures and even after brief exposures to 60°C (Nahar et al., 2013).

Collagen may also be formulated to promote molecular alignment. Thus, nanocrystalline cellulose supplemented to a collagen solution undergoing gelation promoted the aggregation of aligned collagen fibrils of about 35 nm in diameter (Rudisill et al., 2015). Collagen may also be induced to become microfibrillar- comprising monomer aggregates totaling 30 nm or less in diameter (e.g. Fig. 6). Agents including calcium, sucrose, glycerol, and polyethylene glycols, and in some cases low temperature promotes the fibrillar to microfibrillar transition (Prior et al., 2001). Microfibrillar collagen suspensions may be homogeneous, gel-like, and flowable, making them amenable to alignment technologies. In contrast, fibrillar collagen suspensions are often non-homogeneous, insoluble/fibrous, and non-flowable, and thus unsuitable for alignment (Fig. 6). Notably, the commercial application of collagen alignment is being pioneered by Fibralign, Inc. Their product in development- Biobridge™ – is a thread-like scaffold of aligned collagen fibrils to be implanted in patients suffering from secondary lymphedema, a lymphatic drainage disorder caused for example, by cancer surgery and radiation therapy. Biobridge™ is proposed to channel cellular regeneration of the lymphatic system.

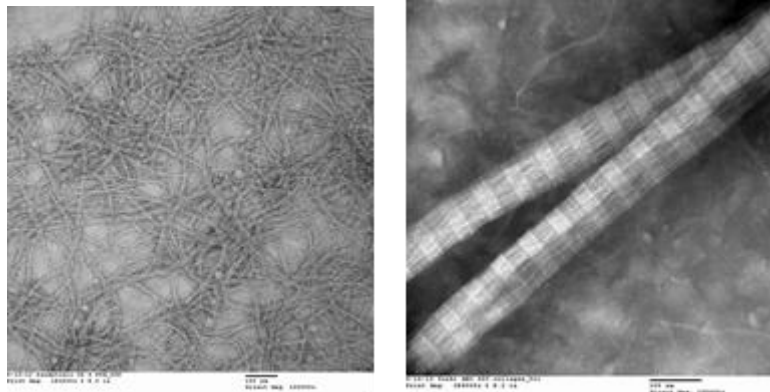


Figure 6. TEM micrographs of Stryker collagen solution A) phosphate precipitated at 4oC comprised of micro-fibrils < 13 nm diameters; B) PBS precipitated at 30oC comprised of native, inter-mediate-sized fibrils of approximately 90 nm diameters (EM performed by Doug Keene).

Someday, collagen alignment technologies may create robust collagen scaffolds of geometries and physical properties approaching those of native tissues. *In vivo* collagen fibrils range in diameters from about fifteen to hundreds of microns, may be aligned, packed at high densities and crosslinked together, or loosely packed and randomly oriented, depending on tissue function. In some tissues fibrils may branch or exhibit structural heterogeneity, such as crimping, at about 100 micron intervals (Franchi et al., 2007). In general, connective tissue strength positively correlates with the diameters of its collagen fibrils (Parry et al., 1978). Thus, formulations need to be developed to create collagen fibrils of specific diameters, and to orchestrate when during scaffold fabrication the fibrils polymerize. For example, larger diameter fibrils may be obtained if collagen oligomers are kept at low concentrations relative to that of monomers. To control polymerization timing, microfibrillar collagen may be aligned via hydrodynamic flow, extruded layer upon layer to form a device, then further polymerized by phosphate precipitation. Polymerization rates and extents may be adjusted depending on whether pepsinized or non-pepsinized collagen is used or lanthanides included. During scaffolding, removal of liquid from the collagen formulation could promote close fibril apposition, and chemical or enzymatic crosslinking applied when desired. Interestingly, methods for collagen alignment could possibly best be achieved via another emerging technology: 3D bioprinting.

11 – 3D Bioprinting: “Cross-over” technology for collagen-based medical device manufacturing

Three-dimensional (3D) printing, also called rapid prototyping or additive manufacturing, emerged from the stereolithography (SLA) method invented by Chuck Hull (founder, 3D Systems) in 1983. Print designs are created with a computer-aided design (CAD), used by the software that transfers into a layer-by-layer print sequence used by a materials printer nozzle that, for example, melt extrudes synthetic materials, pressure-extrudes biologics, or laser sinters powdered material to fabricate the 3D structure. The 3D printing industry has grown significantly since its debut, with the market expected to approach US \$11 billion by 2021 (Jason and Ray, 2013). Currently there are hundreds of 3D printing companies, but a small fraction are established manufacturers. Of these, only four are publically traded, including Arcam, 3D systems, Stratasys and Ex One, all of which supply printers capable of fabricating synthetic devices at high resolution and speed. As example, the Fab@Home printer is a build-it-yourself, desktop printer with printer heads available for synthetics melt-extrusion or syringe-based biologics extrusion (Malone and Lipson, 2007). Table I provides examples of synthetic and biologic printers with select specifications.

3D printing of biologics and living cells has been explored since the early 2000's. Currently there are about 20 companies specializing in bioprinting (<http://stemcellassays.com/2014/07/20-bioprinting->

companies/), and the field is actively being explored in research labs around the world. Many aim to print living organs or tissue-specific scaffolds either for transplantation into humans, or for use in the medical diagnostics; e.g., a living skin-like construct for testing cosmetics toxicity. Biofabrication, the process of artificially building living tissues, has been developing for over a decade, however, the engineering of printers and formulation of bioinks capable of producing viable tissue-like structures is in its infancy. Ideal scaffolds should be biocompatible, biodegradable, and able to promote cell-cell and cell-matrix interactions necessary for maintaining tissue-specific properties. For this reason, cells are encapsulated within a bioink and printed to create a 3D scaffold to support better viability and function as compared with 2D environments such as cell monolayers in tissue culture(Gu, 2015).

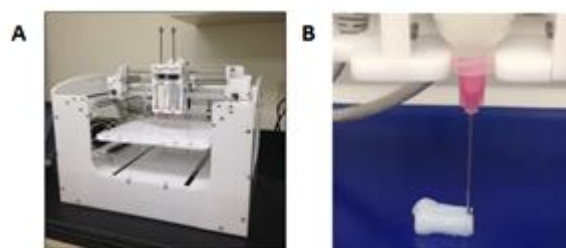


Figure 7. (A) Fab@Home printer outfitted with biologics (syringe extrusion) nozzles; (B) Printing of collagen scaffold.

Table 1. 3D printers and specifications used for synthetic and biological scaffold fabrication.

Model	Manufacturer	Price	Resolution	Print Materials
Cubify Cube Proa	3D Systems	\$2799	100 micron	PLA, ABS, Dissolvable natural PLA
Ultimaker 2^a	Ultimaker	\$2499	20 micron	PLA, ABS, U-PET
Makerbot Replicator^a	Stratasys Ltd	\$2899	100 micron	PLA
Fab@Home (Malone and Lipson, 2007)	Seraph Robotics	\$2500	100 micron	Synthetics and Biologics, UV light tool available
BioBots^b	Biobots	\$5000	100 micron	Biologics modified with proprietary photo curable agent
3D Bioplotter Manufacturer Series^c	EnvisionTec	\$250000	1 micron	Synthetics and biologics, UV light tool available
NovoGen MMX Bioprinter^d	Organovo	Academic Only	Not listed	Biologics

^a<http://3d-printers.toptenreviews.com/>; ^b<http://3dprint.com/19305/biobots-3d-bioprinter/>;

^c<http://envisiontec.com/3d-printers/3d-bioplotter/manufacturer-series/>;

^d<http://www.organovo.com/company/history>

Polymers are attractive materials for 3D printing because unlike metals and ceramics, some may impart structural flexibility, biocompatibility, and bioresorbability to constructs. Two categories of polymers are used in bioprinting: synthetics (e.g., poly (L-lactic acid); PLA, polyglycolic acid; PGA, co-polymers thereof; PLGA, and polycaprolactone, PCL) and biopolymers (e.g., collagen, gelatin, and alginate, an algal polysaccharide). Advantages of synthetics include their reproducibility, controlled mechanical properties, commercial availability and low cost; however, naturally-derived materials are desirable for medical devices because they may provide a more natural chemistry and architecture for biological integration and tissue remodeling (Liu and Ma, 2004). To date, the synthetic polymers PLA and PLGA have been FDA approved for specific clinical applications, and are being used as orthopedic implants and scaffolds (Saito et al., 2013). These polymers differ from each other in degradation time, hydrophilicity, and can have different effects on cell behavior (Saito et al., 2013). The 3D printed porous PLGA scaffolds have been tested both *in vitro* and *in situ* in a rabbit model, and have exhibited good biocompatibility and osteoconductivity (Ge et al., 2009).

Despite these successes, 3D printing of biologics continues to present technical challenges that relate to the delicate structure-function attributes of the materials. As an example, the formulation of certain biomaterials requires them to remain extrudable and/or gel-like as well as compatible with living cells. Moreover, the bioink must assume its target structural complexity/architecture such as firmness, shape, and porosity in the finished device. Another challenge is that typically the 3D printing of plastics and metals requires the material to be melt-extruded or laser sintered and then cooled. This approach is not possible for biopolymers, since most biologics denature above physiologic temperatures. Thus, current attempts involving polymerization/gelation of collagen, gelatin, or alginate, have yielded gels that are not very robust or stable, requiring the addition of curing agents. To address these challenges, BioBot's 3D printer includes a proprietary polymer and photo-initiator to be combined with biomaterials and living cells; exposure of these constituents to ultraviolet light during printing cures the construct to yield a high resolution (80 μm) print and robust construct. Others have developed a hydrogel to be used in 3D printing that is curable by visible light rather than by water-insoluble photoinitiators or ultraviolet light to optimize fabrication with live cells (Lin et al., 2014). Through this approach, the authors used 3D printing to support articular cartilage repair by delivering chondroprogenitor cells encapsulated in a biodegradable methacrylated gelatin-based hydrogel (Lin et al., 2014).

Collagens are potentially the most ideal components for biologic 3D printing formulations owing to their biocompatibility, bioactivity, conformational flexibility, robust structure, availability in numerous processed forms, and low cost. Thus, flowable solutions of denatured and/or hydrolyzed collagen (gelatin), microfibrillar native collagen, particulate crosslinked or non-crosslinked gelatin, limed collagen or native fibrillar collagens may be formulated, each with distinctive physical and biological attributes. Native forms of collagens tend to be more robust and stable than many other proteins and are insensitive to most proteases. Moreover, some collagen may be manipulated to remain soluble during 3D printing but undergo gelation or polymerization afterwards. To date, 3D bioprinting of collagen has mainly been explored on a small-scale in labs for various non-commercial applications. For example, a computerized axial tomography scan of a patient's tissue of interest was used to create a 3D device template and to 3D print a synthetic mold for casting an anatomically exact tissue substitute. The mold was filled with a high density pepsinized collagen gel containing living cells (Liu et al., 2008). One challenge for all but very thin scaffolds, is to provide internal porosity and avenues for capillary network integration, with channels of approximately 100 μm in diameter for cell migration and 300 μm for tissue ingrowth and nutrient diffusion (Saito et al., 2013); notably, such porosity is achievable by most 3D printers. Nonetheless, the above-described collagen formulation was frozen to create ice crystals, which, when evacuated during lyophilization, created the requisite channels. Such scaffolds were used to support human mesenchymal stem cell attachment and proliferation *in vitro* (Liu et al., 2008). Others developed a formulation of porcine gelatin, dissolved in an alginate solution to obtain a product that, when cross-linked post-print with calcium, maintained its geometry and mechanical integrity. This formulation was combined with porcine aortic valve interstitial and smooth muscle cells to print the valve root and leaflet components of an aortic valve conduit. Lastly, others used a collagen hydrogel made from 3.0 mg/mL phosphate precipitated acid soluble rat tail collagen as a scaffold for keratinocytes and fibroblasts (Lee et al., 2014), to print a dermis substitute. Before printing, nebulized sodium bicarbonate vapor was applied to the print surface to enable quick gelation and increased adhesion of the print formulation to the surface. As the vapor was added upon each printed layer, and one minute holds were placed on the print to ensure gelation of each layer prior to the printing of the subsequent layer to yield a firm scaffold.

For optimal collagen bioprinting, we propose that some printers and their bioinks be designed to function as "aligned collagen extruders". Such printers would deliver, via single or multiple printer nozzles, continuous streams of collagen aggregates of various diameters and hundreds, or even thousands to hundreds of thousands of microns long, and to deposit them into desired patterns to form medical devices. Fine tuning the rates of collagen polymerization, fibril diameters, extents of fibril apposition and crosslinking, combined with incorporating "boutique" recombinant collagens with novel structural and biologic activities, would undoubtedly contribute to the diversity and utility of

next generation collagen-based medical devices. Notably, such devices should be fabricated with the requisite dimensions and porosity to enable vascular invasion and metabolic support, and to hasten *in vivo* remodeling when desired. An outstanding hurdle for the 3D bioprinting industry remains to develop print formulations, equipment, and manufacturing methods capable of reproducing scaffolds that meet the rigorous quality requirements of the biotechnology industry and government regulatory agencies, and likewise satisfy the requisite *in vivo* qualities.

12 – Recombinant collagen technology

Someday, recombinant DNA technology promises to create novel collagens for the medical device industry and beyond. This technology has already been used to express collagens in yeast, corn, silkworm cocoons, and tobacco plants, where they normally never exist. Potential benefits include high volume, low cost manufacturing, eliminating the risk of pathogens that may co-purify with collagen isolated from mammalian sources, avoiding the use of animals in the production process, and the ability to manufacture genetically engineered “boutique” collagens with novel attributes. In general, recombinant collagens destined for medical devices would be engineered to be non-immunogenic, and further modified. To repair heart attack-damaged tissues, one might deliver a collagen scaffold endowed with a heightened ability to promote blood vessel regeneration, containing multiple $\alpha 1B2$ integrin binding sites that ligate and stimulate endothelial cells to build capillaries. A collagen for injection to plump lips or smooth skin wrinkles might be engineered to bind extra water and last longer in the body by increasing the extent of carbohydrate modification and number of intermolecular crosslinks, and removing the MMP-1 protease remodeling sequence. In engineered collagens, care would be taken to avoid modifying sequences shown critical for collagen function based on our human mutation mapping studies. Thus, our understanding of the biology of the most prevalent proteins in the vertebrate body, combined with advances in manufacturing medical devices and recombinant technology, are leading us into an exciting future for translational medicine and science.

13 – References

1. Abou Neel, E.A., L. Bozec, J.C. Knowles, O. Syed, V. Mudera, R. Day, and J.K. Hyun. 2013. Collagen--emerging collagen based therapies hit the patient. *Advanced drug delivery reviews*. 65:429-456.
2. Barrea, R.A., O. Antipova, D. Gore, R. Heurich, M. Vukonich, N.G. Kujala, T.C. Irving, and J.P. Orgel. 2014. X-ray micro-diffraction studies on biological samples at the BioCAT Beamline 18-ID at the Advanced Photon Source. *Journal of synchrotron radiation*. 21:1200-1205.
3. Basil-Jones, M.M., R.L. Edmonds, S.M. Cooper, and R.G. Haverkamp. 2011. Collagen fibril orientation in ovine and bovine leather affects strength: a small angle X-ray scattering (SAXS) study. *Journal of agricultural and food chemistry*. 59:9972-9979.
4. Brodsky, B., and A.V. Persikov. 2005. Molecular structure of the collagen triple helix. *Advances in protein chemistry*. 70:301-339.
5. Chapman, J.A. 1974. The staining pattern of collagen fibrils. I. An analysis of electron micrographs. *Connect. Tiss. Res.* 2:137-150.
6. Covington, A.D. 2009. *Tanning chemistry : the science of leather*. Royal Society of Chemistry, Cambridge, UK. xxxi, 483 p. pp.
7. Evans, C.H., and B.J. Drouven. 1983. The promotion of collagen polymerization by lanthanide and calcium ions. *The Biochemical journal*. 213:751-758.
8. Fernandes, R.J., A.W. Farnand, G.R. Traeger, M.A. Weis, and D.R. Eyre. 2011. A role for prolyl 3-hydroxylase 2 in post-translational modification of fibril-forming collagens. *The Journal of biological chemistry*. 286:30662-30669.

9. Franchi, M., A. Trire, M. Quaranta, E. Orsini, and V. Ottani. 2007. Collagen structure of tendon relates to function. *TheScientificWorldJournal*. 7:404-420.
10. Friess, W. 1998. Collagen--biomaterial for drug delivery. *European journal of pharmaceutics and biopharmaceutics : official journal of Arbeitsgemeinschaft fur Pharmazeutische Verfahrenstechnik e.V.* 45:113-136.
11. Gautieri, A., A. Redaelli, M.J. Buehler, and S. Vesentini. 2014. Age- and diabetes-related nonenzymatic crosslinks in collagen fibrils: candidate amino acids involved in Advanced Glycation End-products. *Matrix biology : journal of the International Society for Matrix Biology*. 34:89-95.
12. Ge, Z., X. Tian, B.C. Heng, V. Fan, J.F. Yeo, and T. Cao. 2009. Histological evaluation of osteogenesis of 3D-printed poly-lactic-co-glycolic acid (PLGA) scaffolds in a rabbit model. *Biomedical materials*. 4:021001.
13. Gu, Q.I. 2015. Three dimensional bio-printing. *Science China Life Sciences*. 58.5:411-419.
14. Hay, E.D. 1991. Cell Biology of Extracellular Matrix. Plenum Press, New York and London.
15. Heidemann, E. 1988. The Chemistry of Tanning. In Collagen. Vol. III, Biotechnology. M. Nimni, editor. CRC Press, Boca Raton, FL. 39-61.
16. Hu, X.W., D.P. Knight, and J.A. Chapman. 1997. The effect of non-polar liquids and non-ionic detergents on the ultrastructure and assembly of rat tail tendon collagen fibrils in vitro. *Biochimica et biophysica acta*. 1334:327-337.
17. Hudson, D.M., and D.R. Eyre. 2013. Collagen prolyl 3-hydroxylation: a major role for a minor post-translational modification? *Connective tissue research*. 54:245-251.
18. Iruela-Arispe, M.L., C.A. Diglio, and E.H. Sage. 1991. Modulation of extracellular matrix proteins by endothelial cells undergoing angiogenesis in vitro. *Arterioscler. Thrombos*. 11:805-815.
19. Isobe, Y., T. Kosaka, G. Kuwahara, H. Mikami, T. Saku, and S. Kodama. 2012. Oriented collagen scaffolds for tissue engineering. *Materials*. 5:501-511.
20. Jason, L.T., and T. Ray. 2013. The 3D printed supply chain. *Defense Transportation Journal*.
21. Jiang, F., H. Horber, J. Howard, and D.J. Muller. 2004. Assembly of collagen into microribbons: effects of pH and electrolytes. *Journal of structural biology*. 148:268-278.
22. Kadler, K.E., C. Baldock, J. Bella, and R.P. Boot-Handford. 2007. Collagens at a glance. *J Cell Sci*. 120:1955-1958.
23. King, G., E.M. Brown, and J.M. Chen. 1996. Computer model of a bovine type I collagen microfibril. *Protein engineering*. 9:43-49.
24. Komanowsky, M., H.I. Sinnamon, S.S. Elias, W.K. Heiland, and N.C. Aceto. 1978. Production of comminuted collagen for novel applications. *J. Amer. Leather Chemists Assoc*. 69:410-422.
25. Lee, V., G. Singh, J.P. Trasatti, C. Bjornsson, X. Xu, T.N. Tran, S.S. Yoo, G. Dai, and P. Karande. 2014. Design and fabrication of human skin by three-dimensional bioprinting. *Tissue engineering. Part C, Methods*. 20:473-484.
26. Lehto, M., T.J. Sims, and A.J. Bailey. 1985. Skeletal muscle injury--molecular changes in the collagen during healing. *Research in experimental medicine. Zeitschrift fur die gesamte experimentelle Medizin einschliesslich experimenteller Chirurgie*. 185:95-106.
27. Lin, H., A.W. Cheng, P.G. Alexander, A.M. Beck, and R.S. Tuan. 2014. Cartilage tissue engineering application of injectable gelatin hydrogel with in situ visible-light-activated gelation capability in both air and aqueous solution. *Tissue engineering. Part A*. 20:2402-2411.
28. Liu, C.Z., Z.D. Xia, Z.W. Han, P.A. Hulley, J.T. Triffitt, and J.T. Czernuszka. 2008. Novel 3D collagen scaffolds fabricated by indirect printing technique for tissue engineering. *Journal of biomedical materials research. Part B, Applied biomaterials*. 85:519-528.
29. Liu, X., and P.X. Ma. 2004. Polymeric scaffolds for bone tissue engineering. *Annals of biomedical engineering*. 32:477-486.
30. Malone, E., and H. Lipson. 2007. Design and development of three-dimensional scaffolds for tissue engineering. *Rapid Prototyping Journal*. 13.4:245-255.

31. Marini, J.C., A. Forlino, W.A. Cabral, A.M. Barnes, J.D. San Antonio, S. Milgrom, J.C. Hyland, J. Korkko, D.J. Prockop, A. De Paepe, P. Coucke, S. Symoens, F.H. Glorieux, P.J. Roughley, A.M. Lund, K. Kuurila-Svahn, H. Hartikka, D.H. Cohn, D. Krakow, M. Mottes, U. Schwarze, D. Chen, K. Yang, C. Kuslich, J. Troendle, R. Dalgleish, and P.H. Byers. 2007. Consortium for osteogenesis imperfecta mutations in the helical domain of type I collagen: regions rich in lethal mutations align with collagen binding sites for integrins and proteoglycans. *Hum Mutat.* 28:209-221.
32. Meyer, M., and M. Schropfer. 2013. Collagen-materials- collagen processing. Technical freedom and scientific challenges when transforming collagen into final materials. *Proc. of the XXXII IULTCS Congress, May 2013, Istanbul:*2-16.
33. Morello, R., T.K. Bertin, Y. Chen, J. Hicks, L. Tonachini, M. Monticone, P. Castagnola, F. Rauch, F.H. Glorieux, J. Vranka, H.P. Bachinger, J.M. Pace, U. Schwarze, P.H. Byers, M. Weis, R.J. Fernandes, D.R. Eyre, Z. Yao, B.F. Boyce, and B. Lee. 2006. CRTAP is required for prolyl 3- hydroxylation and mutations cause recessive osteogenesis imperfecta. *Cell.* 127:291-304.
34. Murthy, N.S. 1984. Liquid crystallinity in collagen solutions and magnetic orientation of collagen fibrils. *Biopolymers.* 23:1261-1267.
35. Nahar, Q., D.M. Quach, B. Darvish, H.A. Goldberg, B. Grohe, and S. Mittler. 2013. Orientation distribution of highly oriented type I collagen deposited on flat samples with different geometries. *Langmuir : the ACS journal of surfaces and colloids.* 29:6680-6686.
36. Oliveira, H.C., A.F. Popi, A.L. Bachi, S. Nonogaki, J.D. Lopes, and M. Mariano. 2010. B-1 cells modulate the kinetics of wound-healing process in mice. *Immunobiology.* 215:215-222.
37. Orgel, J.P., and T.C. Irving. 2014. Advances in Fiber Diffraction of Macromolecular Assemblies. *In Encyclopedia of Analytical Chemistry.* John Wiley & Sons.
38. Orgel, J.P., T.C. Irving, A. Miller, and T.J. Wess. 2006. Microfibrillar structure of type I collagen in situ. *Proceedings of the National Academy of Sciences of the United States of America.* 103:9001-9005.
39. Orgel, J.P., A.V. Persikov, and O. Antipova. 2014. Variation in the helical structure of native collagen. *PloS one.* 9:e89519.
40. Orgel, J.P., J.D. San Antonio, and O. Antipova. 2011. Molecular and structural mapping of collagen fibril interactions. *Connective tissue research.* 52:2-17.
41. Orgel, J.P., T.J. Wess, and A. Miller. 2000. The in situ conformation and axial location of the intermolecular cross-linked non-helical telopeptides of type I collagen. *Structure.* 8:137-142.
42. Osaki, S. 1999. Distribution map of collagen fiber orientation in a whole calf skin. *The Anatomical record.* 254:147-152.
43. Ottani, V., M. Raspanti, and A. Ruggeri. 2001. Collagen structure and functional implications. *Micron.* 32:251-260.
44. Parkin, J., J. Savige, J. San Antonio, and a. et. Human type III collagen interactome. *In Preparation.*
45. Parry, D.A., G.R. Barnes, and A.S. Craig. 1978. A comparison of the size distribution of collagen fibrils in connective tissues as a function of age and a possible relation between fibril size distribution and mechanical properties. *Proceedings of the Royal Society of London. Series B, Biological sciences.* 203:305-321.
46. Pepin, M., U. Schwarze, A. Superti-Furga, and P.H. Byers. 2000. Clinical and genetic features of Ehlers-Danlos syndrome type IV, the vascular type. *The New England journal of medicine.* 342:673-680.
47. Persikov, A.V., and B. Brodsky. 2002. Unstable molecules form stable tissues. *Proceedings of the National Academy of Sciences of the United States of America.* 99:1101-1103.
48. Persikov, A.V., J.A. Ramshaw, and B. Brodsky. 2000. Collagen model peptides: Sequence dependence of triple-helix stability. *Biopolymers.* 55:436-450.
49. Persikov, A.V., J.A. Ramshaw, and B. Brodsky. 2005. Prediction of collagen stability from amino acid sequence. *The Journal of biological chemistry.* 280:19343-19349.
50. Piez, K.A., and A.H. Reddi. 1984. Extracellular Matrix Biochemistry. Elsevier, New York.

51. Prior, J.P., D.G. Wallace, D.H. Sierra, and F.A. DeLustro. 2001. Compositions containing thrombin and microfibrillar collagen and methods for preparation and use thereof. USPTO, editor. Cohesion Technologies, Inc., US.
52. Prockop, D.J., and A. Fertala. 1998. Inhibition of the self-assembly of collagen I into fibrils with synthetic peptides. Demonstration that assembly is driven by specific binding sites on the monomers. *J. Biol. Chem.* 273:15598-15604.
53. Rainey, J., and M. Goh. 2002. A statistically derived parameterization for the collagen triple-helix. *Protein Sci.* 11:2748-2754.
54. Reigle, K.L., G. Di Lullo, K.R. Turner, J.A. Last, I. Chervoneva, D.E. Birk, J.L. Funderburgh, E. Elrod, M.W. Germann, C. Surber, R.D. Sanderson, and J.D. San Antonio. 2008. Non-enzymatic glycation of type I collagen diminishes collagen-proteoglycan binding and weakens cell adhesion. *J Cell Biochem.*
55. Rong, Y.H., G.A. Zhang, C. Wang, and F.G. Ning. 2008. [Quantification of type I and III collagen content in normal human skin in different age groups]. *Zhonghua shao shang za zhi = Zhonghua shaoshang zazhi = Chinese journal of burns.* 24:51-53.
56. Rudisill, S.G., M.D. DiVito, A. Hubel, and A. Stein. 2015. In vitro collagen fibril alignment via incorporation of nanocrystalline cellulose. *Acta biomaterialia.* 12:122-128.
57. Saito, E., E.E. Liao, W.W. Hu, P.H. Krebsbach, and S.J. Hollister. 2013. Effects of designed PLLA and 50:50 PLGA scaffold architectures on bone formation in vivo. *Journal of tissue engineering and regenerative medicine.* 7:99-111.
58. San Antonio, J.D., M.H. Schweitzer, S.T. Jensen, R. Kalluri, M. Buckley, and J.P. Orgel. 2011. Dinosaur peptides suggest mechanisms of protein survival. *PloS one.* 6:e20381.
59. Scott, J.E. 1988. Proteoglycan-fibrillar collagen interactions. *Biochem. J.* 252:313-323.
60. Stachel, I., U. Schwarzenbolz, T. Henle, and M. Meyer. 2010. Cross-linking of type I collagen with microbial transglutaminase: identification of cross-linking sites. *Biomacromolecules.* 11:698-705.
61. Svensson, R.B., H. Mulder, V. Kovanen, and S.P. Magnusson. 2013. Fracture mechanics of collagen fibrils: influence of natural cross-links. *Biophysical journal.* 104:2476-2484.
62. Swamy, R.N., A. Gnanamani, S. Shanmugasamy, R.K. Gopal, and A.B. Mandal. 2011. Bioinformatics in crosslinking chemistry of collagen with selective cross linkers. *BMC research notes.* 4:399.
63. Sweeney, S.M., J.P. Orgel, A. Fertala, J.D. McAuliffe, K.R. Turner, G.A. Di Lullo, S. Chen, O. Antipova, S. Perumal, L. Ala-Kokko, A. Forlino, W.A. Cabral, A.M. Barnes, J.C. Marini, and J.D. San Antonio. 2008. Candidate cell and matrix interaction domains on the collagen fibril, the predominant protein of vertebrates. *The Journal of biological chemistry.*
64. Whitford, C., H. Studer, C. Boote, K.M. Meek, and A. Elsheikh. 2015. Biomechanical model of the human cornea: considering shear stiffness and regional variation of collagen anisotropy and density. *Journal of the mechanical behavior of biomedical materials.* 42:76-87.
65. Wood, G.C., and M.K. Keech. 1960. The formation of fibrils from collagen solutions. 1. The effect of experimental conditions: kinetic and electron-microscope studies. *The Biochemical journal.* 75:588-598.